https://doi.org/10.1016/j.trechm.2024.10.004

Stable MOFs and composites for photocatalytic antibacterial applications

Si Ma[1,2], Yintung Lam[3], Le Shi[1,2], Kaikai Ma[3]* and Zhijie Chen[1,2]*

[1]*Stoddart Institute of Molecular Science, Department of Chemistry, Zhejiang Key Laboratory of Excited-State Energy Conversion and Energy Storage, State Key Laboratory of Silicon and Advanced Semiconductor Materials, Zhejiang University, Hangzhou 310058, P. R. China*

[2]*Zhejiang-Israel Joint Laboratory of Self-Assembling Functional Materials, ZJU-Hangzhou Global Scientific and Technological Innovation Center, Zhejiang University, Hangzhou 311215, P. R. China*

[3]*School of Fashion and Textiles, The Hong Kong Polytechnic University, Hung Hom, Hong Kong, SAR, China*

*Corresponding author. Email: zhijiechen@zju.edu.cn; kaikai.ma@polyu.edu.hk

MAIN TEXT

Abstract

Photocatalytic sterilization is regarded as an attractive solution to combat the threats brought by infectious pathogens. Recently, metal-organic frameworks (MOFs) with controllable designability and tunable functionality have emerged as desirable candidates to fabricate photocatalytic sterilizers. This review systematically summarizes the latest progress on MOF-based materials developed for photocatalytic sterilization. It mainly focuses on the antimicrobial mechanism, evaluation methods of stable MOFs as well as their prospective practical applications. In addition, diverse strategies toward the design and synthesis of high-performance antimicrobial MOFs are discussed. Finally, the challenges and future perspectives in this progressing and thriving field are highlighted. This review aims to provide an insight into the design of MOF-based photoactive platforms, and facilitate development of photocatalytic antibacterial arsenals.

Using MOFs for photocatalytic sterilization

Infectious pathogens, including bacteria, fungi and viruses, inevitably pose negative impact on human life and health, public safety, as well as social and economic development[1]. For example, the sudden and rapid outbreak of corona virus disease 2019 (COVID-19) brought indelible harm to humans all over the world. Lots of patients and the elderly with weakened immune systems died from pathogenic infections, complications or even secondary bacterial infection[2]. Besides, other emerging and re-emerging diseases, like influenza, measles and severe acute respiratory syndrome, endanger the health of humankind[3].

It is worth noting that metal, carbon and other electroactive materials have been widely used for sterilization purposes, but they often have limited antimicrobial resistance and require complex operations[4]. Recently, photocatalytic antibacterial approaches have gained much attention, because light-induced reactive oxygen species (ROS) generated from the photocatalysts are recognized to be very efficient, clean and sustainable disinfectants. The highly oxidative ROS can damage the cell membrane and

organelle of microbes, inactivating or even killing the microbes[2]. Generally, different photocatalysts harvest distinct light energy for ROS generation [5,6]. Conventional inorganic antimicrobial agents, like metal oxides and metal sulfides, mostly possess large band gaps and they are unable to utilize visible light for generating ROS. Their relatively smaller surface areas also impede the fast production of ROS[2]. In addition, high cost of metal nanoparticles like Pt and Au limit their large-scale use[2]. Therefore, high-performance and low-cost photocatalysts are in high demand.

Metal-organic frameworks (MOFs), constructed from organic and inorganic metal building blocks, are extensively studied for their potential as photocatalysts owing to their diverse designability and tunable functionality[7-9]. Recently, MOF-based photocatalysts with low toxicity and ease of functionalization have shown great prospects for biomedical and healthcare applications[10,11]. Their unique features include: (i) porous nature of MOFs allows easy incorporation and uniform distribution of other functional materials[12]; (ii) unsaturated metal sites and substitutable organic blocks of MOFs endow them diverse types of functionalities[13,14]; (iii) fine biocompatibility and biodegradability of MOFs enable them to have wide applicability[15,16]. As such, MOFs are considered as an ideal platform for developing ground-breaking photocatalytic antimicrobial agents for broad applications.

Several reviews in antimicrobial applications, mainly focusing on the introduction of different kinds of antimicrobial materials and their underlying mechanisms[2,6,15-17], have been reported lately. However, there are few reviews highlighting the design and antimicrobial applications of photoinduced ROS-generating MOFs. This review aims to give a comprehensive overview on recent advances in MOF-based materials for photocatalytic sterilization. Firstly, the antimicrobial mechanism and evaluation methods of ROS-generating MOFs are introduced. Then, several representative stable MOFs are highlighted to show their practical potential for air purification, water sterilization, wound dressing and protective equipment such as antibacterial textiles. Furthermore, various approaches for the design and construction of efficient antimicrobial MOFs are illustrated. Finally, we also put forward some existing

challenges in current research and give insights for future directions. We hope that this review will stimulate more researchers' interest in photocatalytic sterilization and provide new viewpoints for designing efficient MOF-based photocatalytic platforms.

Fundamentals of MOF materials for photocatalytic sterilization

Microbial pathogens can survive on various surfaces and carriers like clothing, handles and packaging for several days, making pathogen transmission difficult to control. Therefore, there is an urgent need to develop self-cleaning materials to eliminate pathogens in the human living environment[18,19]. To fully utilize the potential of photosensitive MOFs in practical antimicrobial applications, it is crucial to develop approaches towards fabricating useful items such as protective clothing and equipment with MOF-based composites[20-22]. Generally, MOFs can be integrated into various substrates, including coatings, fibers composites, membrane materials[23,24]. There are two common strategies for synthesizing MOF composites: *in-situ* growth and post-coating method[25]. In the former method, MOF layers could be hydrothermally grown directly onto the frameworks of substrates. Alternatively, in the post-coating method, preformed MOF nanocrystals can be incorporated onto a substrate[25]. The MOF component imparts desirable functionality and reactivity to the substrate, while the substrate ensures excellent processability and flexibility for manufacturing and usage [20,22]. The synergistic combination of MOFs and substrates facilitates the development of MOF-based composites with enhanced performance and efficiency for practical applications[26,27].

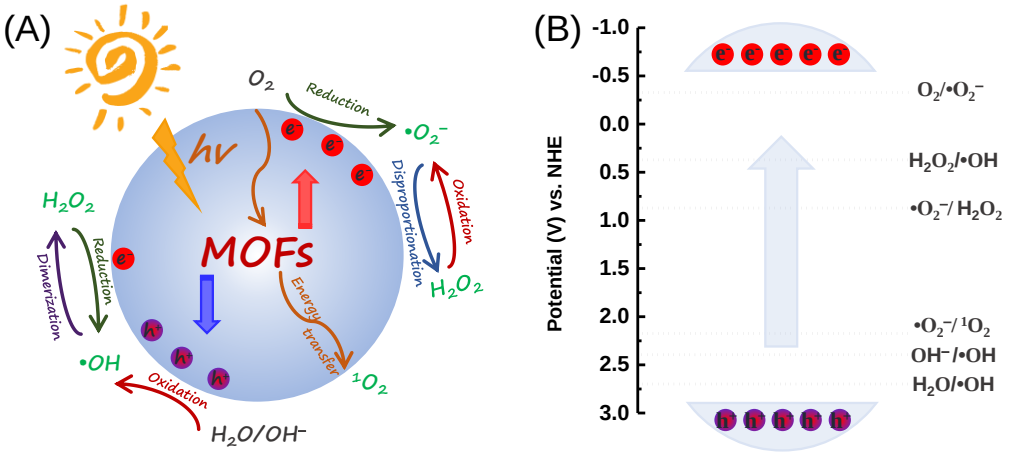

Figure 1. The process (A) and driving force (B) of ROS generation by MOFs.

For the antimicrobial action of MOF-based photocatalysts, ROS-based chemical oxidation is usually the predominant reaction mechanism[15]. Common ROS including the superoxide anion ($\bullet O_2^-$), hydroxyl radical (•OH), singlet oxygen ($^1O_2$), and hydrogen peroxide (H_2O_2) can be regarded as clean oxidants for interfering with the structures or activities of microbes [2]. ROS generation in photocatalysts generally involves three steps: (i) light-triggered charge carrier formation; (ii) charge carrier migration and recombination; (iii) ROS generation at the surface of photocatalysts (**Figure 1A**)[28]. Specifically, photosensitive MOFs are excited under the irradiation of visible light. Electrons (e^-) escape to the conduction band (CB) while holes (h^+) are left in the valence band (VB), resulting in the separation of electron-hole pairs (e^- and h^+, charge carrier). Then, the charge carriers will respectively migrate to reaction sites. It should be noted that some of the charge carriers may recombine, leading to the reduction of free charge carriers for ROS generation. Finally, various ROS are generated through a series of oxidation or reduction reactions initiated by free h^+ and e^- [2,28-30]. In detail, free e^- is trapped by O_2 to generate $\bullet O_2^-$ at CB, and $\bullet O_2^-$ may gradually be converted to H_2O_2 after accepting H^+ and e^-. Simultaneously, the oxidative h^+ reacts with H_2O or OH^- to produce •OH. Distinctively, $^1O_2$ is often formed as a result of energy transfer (**Figure 1A**)[16,31-33]. It is worth noting that these photogenerated ROS can subsequently be converted to another ROS via further oxidation, reduction, disproportionation, or dimerization[28]. Therefore, multiple ROS may play a key role in the oxidative inactivation of pathogens in practical applications[5].

The reactions can usually occur when the band structure of a photocatalyst overlaps with the redox potentials of a photocatalytic reaction[34,35]. MOFs with certain CB and VB can drive the generation of particular ROS [15]. For example, the reduction of O_2 to $\bullet O_2^-$ only occurs when the CB of MOFs is more negative than the potential of $O_2/\bullet O_2^-$, while the oxidation of •OH to H_2O happens when the VB is more positive than the potential of H_2O/•OH (**Figure 1B**)[15]. The CB and VB of typical MOF-based photocatalysts are listed in **Figure 2**, and some of these MOFs with great

potential have yet to be applied in photocatalytic sterilization[36-42].

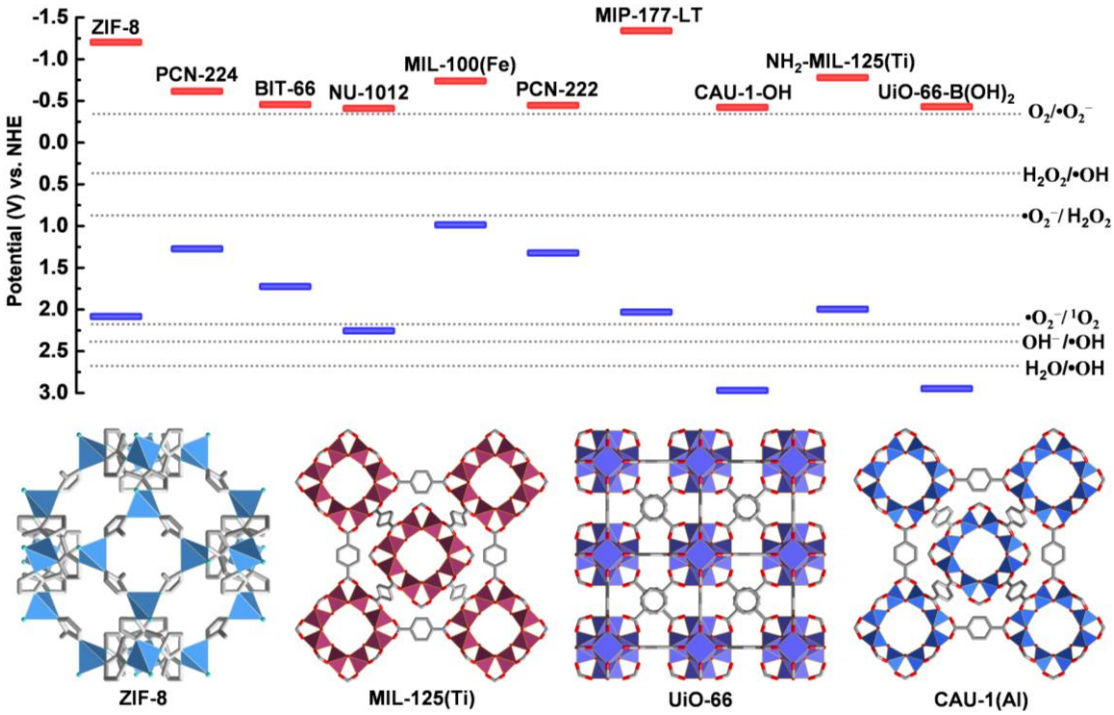

Figure 2. The conduction band and valence band of some typical MOFs[36-42], and the structures of selected representative MOFs.

To evaluate the antimicrobial performance of photoinduced ROS-generating MOFs, Gram-positive bacterial strains like *Staphylococcus aureus* (*S. aureus*), and Gram-negative bacterial strains, like *Escherichia coli* (*E. coli*), are mostly chosen as the representative microbes[16]. In addition, the evaluation is usually divided into *in vivo* and *in vitro*. Evaluation of *in vivo* activity is mostly conducted on experimental murine models, directly observing the differences between the control group and the experimental group[40]. Recently, MOF-based photocatalysts have been applied to *in vivo* photodynamic therapy against bacteria, which is valued as an alternative to traditional antibiotic therapy[2]. For *in vitro* research, the plate counting method is commonly selected to explore *in vitro* antibacterial performance, and the inactivation efficiency is estimated by counting colonies and subsequent statistical analysis[41].

Choosing Stable MOFs for purpose

Considering the fundamentals of MOFs for photocatalytic sterilization, stability

and durability of the chosen photocatalysts are important for practical implementation[43,44]. According to Hard-Soft-Acid-Base (HSAB) theory, stable MOFs are usually fabricated based on the coordinative assembly of hard carboxylate linkers and hard high-valent metal ions like Al^{3+}, Zr^{4+} or Ti^{4+}, or soft azolate ligands and soft transition metal ions such as Zn^{2+} or Cu^{2+}[45,46]. Based on screening and analysis of the existing literature, the remarkable applicability of stable azolate-based Zn-MOFs for sterilization, as well as stable carboxylate-based Al-MOFs, V-MOFs, Zr-MOFs, and Ti-MOFs, are emphasized in this section. The typical stable MOF-based materials and their photocatalytic antibacterial performance are summarized in **Table 1**.

Table 1. Stable MOF-based materials and their photocatalytic antibacterial efficiency

MOFs	Nodes	Linkers	Substrates	Light source	Time	Efficiency	Ref.
ZIF-8	Zn^{2+}	H-MeIM	NWFs	300 W Xe lamp	30 min	> 99.99 %	[39]
ZIF-8	Zn^{2+}	H-MeIM	TPU	Xe lamp	2 h	> 96 %	[47]
MAF-7@4	Zn^{2+}	H-MeIM, Hmtz	PES	300 W Xe lamp	3 h	100 %	[48]
ZnDMZ	Zn^{2+}	H-MeIM	–	660 nm light.	20 min	99.9 %	[49]
AuNR@ZIF-8@AuNC	Zn^{2+}	H-MeIM	Fabrics	Xe lamp	30 min	Almost killed	[50]
ZIF8-SQ	Zn^{2+}	H-MeIM	–	Red light (650 nm)	30 min	86 %	[51]
QDs@ZIF-8	Zn^{2+}	H-MeIM	–	300 W Xe lamp	1 h	7.99 lg reduction	[52]
ZIF-8@iCOF	Zn^{2+}	H-MeIM	PAN	Sunlight	1 h	Almost killed	[53]
CAU-1-OH	Al^{3+}	BDC-OH	NWFs	300 W Xe lamp	30 min	99.6 %	[54]
BIT-66	V^{4+}	H_3BTB	EVA	300 W Xe lamp	1 h	96 %	[55]
PCN-224(Cu)	Zr^{4+}	TCPP	–	Blue light	15 min	99.4 %	[56]
Au/PCN-224/Cu(II)	Zr^{4+}	TCPP	Fabrics	300 W Xe lamp	80 min	Almost 100 %	[57]
Cu_{10}MOF	Zr^{4+}	TCPP	–	660 nm light	20 min	99.71 %	[33]
MOF-545	Zr^{4+}	TCPP	–	White LED	20 min	98 %	[58]
PDINH/NH_2-UiO-66(Zr)	Zr^{4+}	NH_2-BDC	–	100 W LED lamp	4 h	Almost 100 %	[59]
Zr-UiO-66-$B(OH)_2$	Zr^{4+}	H_2BDC-$B(OH)_2$	–	Simulated sunlight	2 h	Almost 100 %	[60]
PB@MOF	Zr^{4+}	BDC	–	660 and 808 nm light	10 min	99.99 %	[61]
UiO-66-	Zr^{4+}	$(SH)_2$-	–	Visible light	–	Almost	[62]

$(SH)_2$@TCPP @AgNPs		BDC				killed	
NU-1012	Zr^{4+}	H_4TBAPy	CT	Simulated daylight	1 h	7-log reduction	[41]
PCN-224(Zr/Ti)	Zr^{4+}	TCPP	PLGA	Visible light	30 min	Obviously reduced	[40]
TCPPCu-BBDC	Zr^{4+}	TCPP, BBDC	–	200 mW cm^{-2}	30 min	~ 98 %	[38]
PDI@-MIL-125(Ti)-NH_2	Ti^{4+}	NH_2-BDC	–	300 W Xe lamp	15 min	> 97 %	[63]
NH_2-MIL-125@DhaTph	Ti^{4+}	NH_2-BDC	–	Visible light	50 min	90.2 %	[64]
NA/NH_2-MIL-125(Ti)	Ti^{4+}	NH_2-BDC	–	100 W LED lamp	1 h	99.999 %	[65]
Ag/NH_2-MIL-125(Ti)	Ti^{4+}	NH_2-BDC	–	10 W LED lamp	25 min	> 7-log reduction	[66]

Abbreviation: H-MeIM = 2-methylimidazole, NWFs = non-woven fabrics, TPU = thermoplastic polyurethane, PES = polyethersulfone, Hmtz = 3-methyl-1,2,4-triazole, BDC-OH = 2-hydroxy-1,4-benzendicarboxylic acid, TCPP = meso-tetra(4-carboxyphenyl)porphyrin, H_3BTB = 1,3,5-tris(4-carboxyphenyl)benzene, EVA = ethylene–vinyl acetate copolymer, NH_2-BDC = 2-aminoterephthalic acid, PDINH = PDI = perylene-3,4,9,10-tetracarboxylic diimide, NA = 1-naphthylamine, SQ = squaraine, BDC = terephthalic acid, BBDC = H_2BDC-$B(OH)_2$ = 2-boronobenzene-1,4-dicarboxylicacid, PAN = polyacrylonitrile, $(SH)_2$-BDC = 2,5-dimercaptoterephthalic acid, H_4TBAPy = 1,3,6,8-tetrakis(*p*-benzoic acid)pyrene, CT = cotton textile, PLGA = poly(lactic-co-glycolic acid), "–" means not provided.

Zeolitic imidazolate frameworks (ZIFs), consisting of transition metal ions and imidazolate linkers, are a subclass of MOFs with good chemical and thermal stability[67]. ZIF-8, also known as MAF-4[68], is assembled from 2-methylimidazolate and Zn^{2+}. With the advantages of high surface area and intrinsic photochemical response[69,70], it is widely applied in photocatalytic hydrogen evolution, environmental remediation, as well as antimicrobial fields. For example, Wang et al. prepared a series of MOFs, including ZIF-8, MIL-100(Fe), NH_2-MIL-125(Ti), NH_2-UiO-66(Zr), and ZIF-11(Zn), for antimicrobial purposes[39]. Among these, ZIF-8 achieves the highest antibacterial efficiency of >99.99% against *E. coli* under simulated solar light irradiation[39]. It should be emphasized that the log inactivation efficiency of ZIF-8 (6-log) outperforms four and three times than those of the conventional counterparts like TiO_2 (2-log) and ZnO (3-log). The mechanism studies reveal that *E. coli* was eliminated by the ROS generated via ligand-to-metal charge transfer rather than Zn^{2+} ion release.

Moreover, a MOF-based composite was fabricated by loading ZIF-8 onto non-woven fabrics, which is suitable for both particulate matter filtration and bacterial inactivation (**Figure 3A**). This study demonstrates the potential of MOFs for producing personal protective equipment (PPE) and paves the way for the application of MOFs in air purification. In another example, Li et al. constructed a hierarchical composite nanofiber membrane with ZIF-8 and polyurethane via electrospinning technology[47]. In a photocatalytic antibacterial experiment, the as-prepared composite membrane exhibits a high killing rate of 96% for bacteria. Benefiting from the scalable and facile manufacturing method, this composite membrane is a promising material for the production of protective textiles[47]. Nevertheless, these research studies lack comprehensive investigation in the biosafety of the MOFs, failing to prove their suitability in healthcare-related settings.

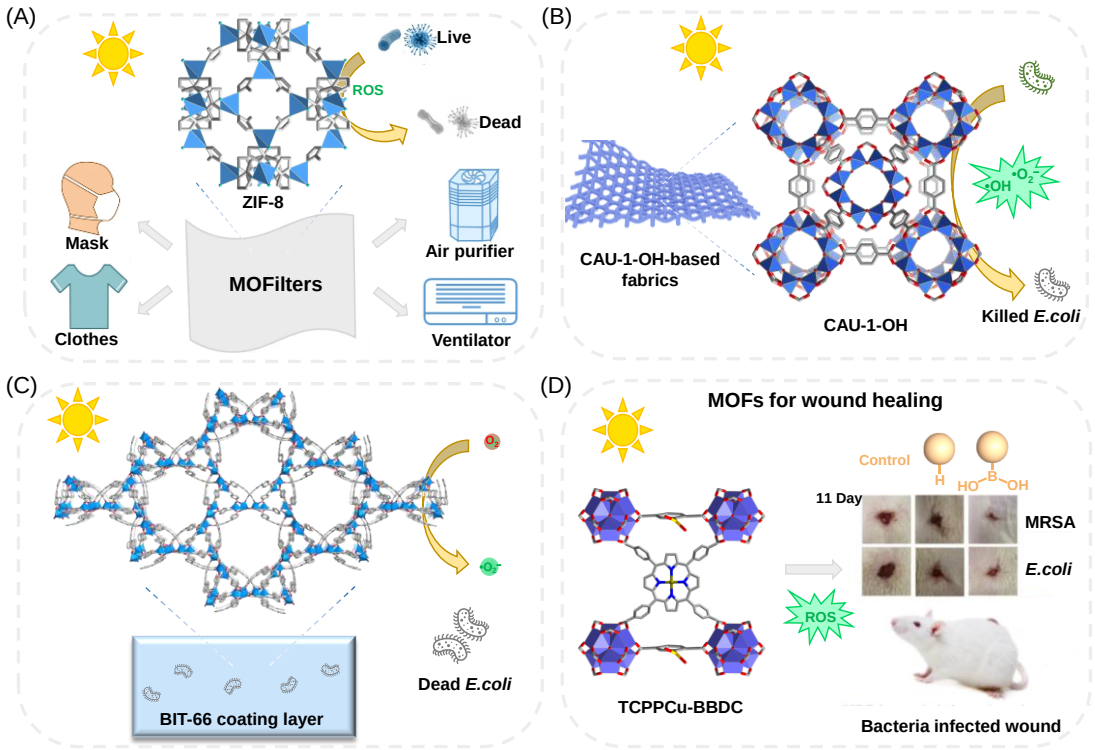

Figure 3. (A) Schematic representation of ZIF-8-based filter for air purification[39]; (B) Schematic diagram of prevention in microbial contamination using a CAU-1-OH-based filter[54]; (C) Schematic illustration of BIT-66 coating layer for photocatalytic bacterial inactivation[55]; (D) Schematic representation of the facile synthesis of multivariate MOFs for synergistic bacterial-binding functions and their practical

application for wound dressing[38]. Adapted, with permission, from [38,39].

Aluminum-based MOFs (Al-MOFs), consisting of organic linkers and Al^{3+} nodes, generally display a high thermal and chemical stability owing to the strong aluminum-oxygen bond[71]. In particular, the abundant sources and low toxicity of Al element enable Al-MOFs to be used for biomedical applications[71]. In 2020, Wang et al. reported a series of Al-MOFs via ligand regulation[54], among which CAU-1-OH exhibits the highest antibacterial activity against *E. coli*. with efficiency up to 99.94% (**Figure 3B**). The quenching study, using sacrificial reagents for reacting with ROS, reveals that •OH, $•O_2^-$ as well as h^+ play a significant role in photocatalytic process. Moreover, a composite was further produced by coating CAU-1-OH onto a commercial nonwoven fabric, which can inactivate airborne bacteria efficiently within 30 minutes under simulated sunlight irradiation. Although Al is considered a biofriendly metal, the overall toxicity of Al-based MOFs in this form is still unknown.

Vanadium-based MOFs (V-MOFs) are structurally robust, attributed to the presence of multivalent vanadium ions ($V^{3+}/V^{4+}/V^{5+}$)[72,73]. Recently, more V-MOFs have been employed as photocatalysts for antibacterial applications, holding a great promise for this purpose[73]. Wang et al. synthesized a stable V^{4+}-MOF (BIT-66) by hydrothermal reaction of VCl_3 and H_3BTB in water[55]. The long-term stability and fast visible-light response endow BIT-66 with exceptional performance in bacteriostatic applications. Specifically, a mixture of activated BIT-66 and ethylene-vinyl acetate copolymer (EVA) was coated on a steel plate to construct a device model. The BIT-66 coating layer irradiated with visible light shows *E. coli* killing efficiency of up to 96% within 1 h (**Figure 3C**), and the antibacterial performance of BIT-66 outperforms that of commercial porous materials like MCM-41. The work not only expands the application fields of V-MOFs but also shows the application prospect of MOFs in air purification[55]. Further prerequisites for practical applications such as stability and durability of this MOF coating layer are yet to be fully explored, but this is a promising start.

Zirconium-based MOFs (Zr-MOFs) are one of the mostly studied MOFs by virtue

of their high thermal, chemical, and hydrolytic stability[74,75]. The highly tunable structures along with the diverse connectivity of Zr-MOFs grant themselves multiple functionalities for various applications, including catalysis, sensing, and water harvesting[76-78]. It is notable that Zr-MOF-based photocatalysts have already been widely employed in photocatalytic sterilization[79-81]. For instance, Jiang et al. constructed a photoactive Zr-MOF by integrating bacterial-binding boronic acid ligands[60] and photosensitive porphyrin Cu(II)[38]. The as-prepared UiO-66-type MOF (TCPPCu-BBDC) exhibits an enhanced antimicrobial activity of 10- to 20-fold higher antibacterial efficiency than Zr-MOF, owing to closer physical contact with bacteria through the boronic acid moieties, as well as more effectual ROS production by Cu^{2+} introduction. The low cytotoxicity of TCPPCu-BBDC suggests high biocompatibility. Besides, *in vivo* experiments demonstrate the capability of the multivariate MOF to shorten the duration for healing a wound in mice infected by drug-resistant bacteria (**Figure 3D**)[38]. This highlights their wide feasibility for biomedical applications such as wound healing and targeted antitumor drugs.

On account of the metal ion coordination site and photosensitivity of porphyrins, Wang et al. have also constructed a series of light-responsive Zr-MOFs (PCN-224(M), M = Fe, Cu, Ag, Zn) based on typical PCN-224(H) through porphyrin metalation[56]. Among these, PCN-224(Cu) shows the highest photoinduced antibacterial activity against *S. aureus* with efficiency of 99.4%. This research provides us a strategy to control the rate of ROS generation by metal doping and promotes the application of MOFs in water sterilization[56]. However, factors affecting its antibacterial mechanism have yet to be fully probed. Considering that metal-doped porphyrin is a strong photosensitizer, the influence of heat generated by porphyrin-based MOFs under light irradiation should also be studied through control experiments.

Titanium-based MOFs (Ti-MOFs) are also considered as attractive photocatalysts thanks to their excellent framework robustness and distinctive photo-redox properties[76]. Their low toxicity and good bioavailability grant Ti-MOFs unique superiority for biological applications[82,83]. Liang et al. prepared a perylene-3,4,9,10-

tetracarboxylic diimide (PDI) bridged Ti-MOFs via a two-step synthesis method, denoted as PDI@MTi[63]. The as-prepared heterostructure can almost kill all bacteria within 15 minutes under visible light irradiation by the synergetic effects of the micro polarization field, bonding interfaces and abundant active sites[63]. This investigation provides a deep insight on the control of carrier separation for acquiring high photocatalytic performance.

We have witnessed the rapid development of MOFs and MOF-based photocatalysts over the last few decades, but their applications in photocatalytic sterilization are still at the early stage. On the one hand, only a limited number of MOFs have been studied for photocatalytic antibacterial applications. More investigations have to be conducted in order to expand the varieties of organic ligands and metal ions, as well as robust synthesis methods for photocatalytic MOFs. Alongside this, the evaluation systems for antibacterial performance require improvements, such as the assessment of durability and biocompatibility of MOFs, standardization and unification of antimicrobial experiments and so on.

Design strategies for improved antibacterial efficiency

As previously reported, we understand that abundant ROS accumulated on the contact surface between photocatalysts and bacteria can greatly improve antibacterial performance[6,84]. Considering the process of ROS generation, desirable photocatalysts should possess the following properties: (i) strong light harvesting ability for enough photoexcitation; (ii) quick separation and migration of charge carrier for large amount of free e^-/h^+; (iii) effective redox reaction for the generation of abundant ROS; and (iv) high surface reaction dynamics for efficient sterilization[2,17]. Some interesting publications on the photocatalytic antibacterial applications of MOF-based materials have been reported in the last decade, in which various strategies are adopted to optimize the antibacterial capacity[16,44]. here, we illustrate these design strategies with relevant recent examples (**Figure 4**).

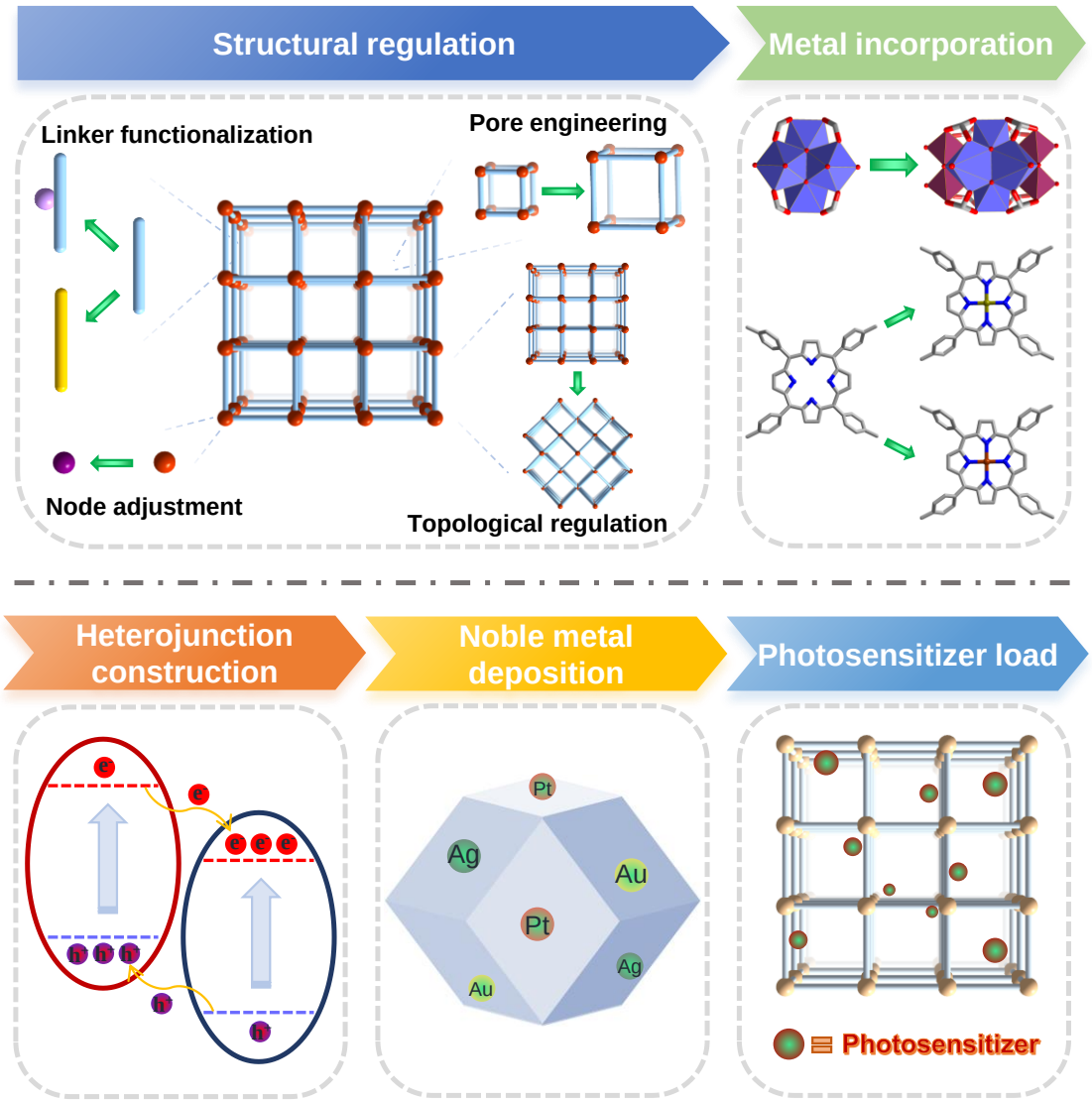

Figure 4. The design strategies of MOFs for improved antibacterial performances. top: structural regulation and metal incorporation; bottom: heterojunction construction, noble metal deposition and photosensitizer load.

The property and functionality of photoactive MOFs can often be regulated by pre-design and post-modification(**Figure 4, top**)[43]. For example, Yan et al. reported an investigation on the influence of topological networks on photocatalytic antibacterial performance[58]. Four porphyrin-based Zr-MOFs with different nets such **ftw**, **csq**, **shp** and **she** were prepared and denoted as MOF-525, MOF-545, PCN-223 and PCN-224, respectively. Among them, MOF-545 causes the most significant damage to *E. coli* and *S. aureus*. In-depth investigation of the results reveals that quicker generation of $^1O_2$ in MOF-545 brings about better antibacterial activity. This can be attributed to a

synergistic effect of larger pore size, more closely packed porphyrin sites and a higher amount of porphyrin per Zr_6O_8 cluster (**Figure 5A**). This study provides a new direction for tuning functionality by the rational design of MOFs[58]. Chemical composition of MOFs can be modified simply by introducing functional molecules. Wang et al. constructed a NA/NH_2-MIL-125(Ti) homojunction by introducing 1-naphthylamine (NA) into the framework of NH_2-MIL-125(Ti) via covalent modification[65]. The introduced chromophore can greatly strengthen the light harvesting abilities as well as promote the separation of charge carrier and generation of ROS, gaining high antibacterial efficiency of 99.99% under the exposure to visible light within 1 hour [65].

Post-synthetic metal incorporation into MOF photocatalysts can amenably modulate their features and functionality[29]. For instance, Wu et al. prepared a series of Cu^{2+} doped PCN-224 by incorporating different amount of Cu^{2+} into the porphyrin unit, and the resulting Cu_{10}MOF shows optimized antibacterial activity with an efficacy of 99.71%[33]. Mechanism analysis demonstrates that the introduction of Cu^{2+} could effectively trap e^-, suppress e^-/h^+ recombination, and accelerate the free carrier transmission for the enhanced ROS production. For *in vivo* application, the Cu_{10}MOF effectuates competent bacterial killing and also assists wound healing[33].

Furthermore, metal nodes of MOFs can also be modified via post-synthetic metal incorporation[44]. Farha et al. reported a Ti-incorporated Zr-pyrene-based MOF, denoted as NU-1012[41]. The introduction of Ti substantially promotes more free carriers for generating abundant ROS, which achieves the aim of improving antibacterial behavior of the MOFs (**Figure 5C**). Additionally, a NU-1012-coated textile with excellent bacteria-killing ability was fabricated by embedding NU-1012 onto cotton cloths via an *in-situ* growth method [41]. This work paves a feasible way to construct high-performance MOF-based antibacterial textiles, but there is a lack of research on the stability and robustness of this composite in practical usage. In a similar vein, Shao et al. designed a bimetallic PCN-224(Zr/Ti) via post-modified metal incorporation to increase the generation of ROS[40]. This was then fabricated into a composite material, produced by the combination of PCN-224(Zr/Ti) and poly(lactic-

co-glycolic acid), which was found to accelerate the healing of infected wounds, suggesting its potential for wound dressing[40].

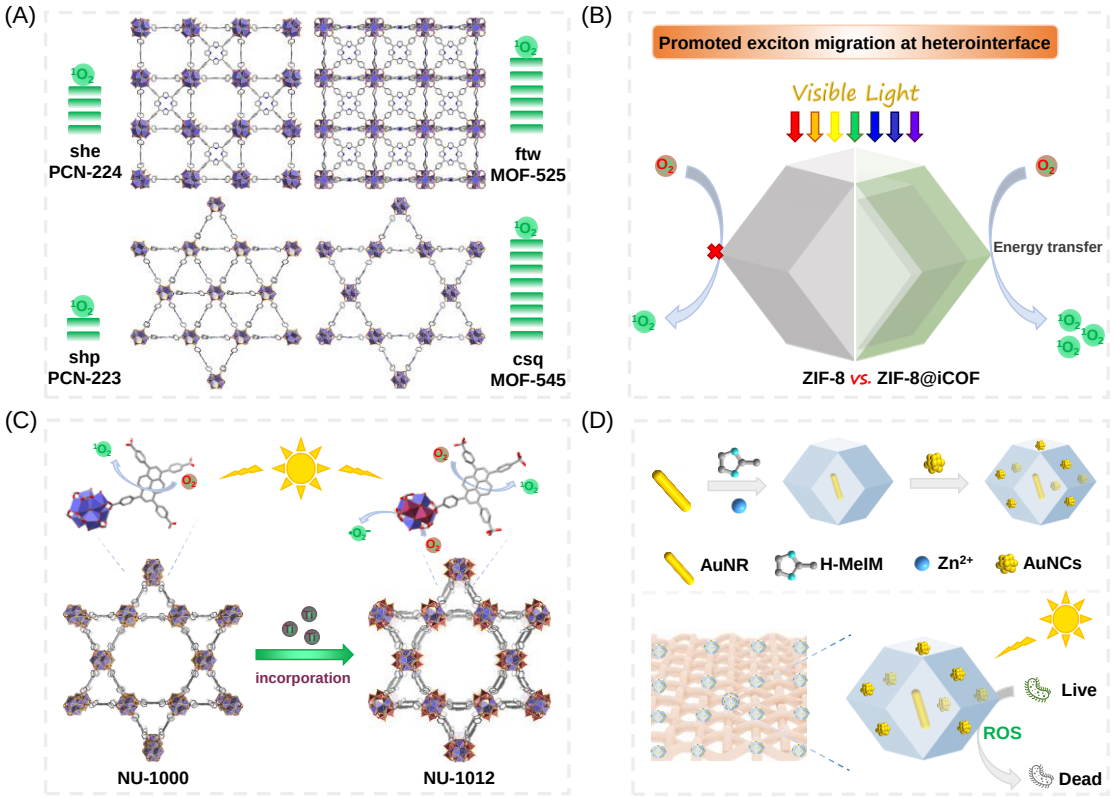

Figure 5. Examples of MOFs designed with different strategies: (A) Porphyrin-based Zr-MOFs and their abilities for generating $^1O_2$[58]; (B) Heterojunction of ZIF-8 and ionic COF, promoting exciton migration at heterointerface for abundant $^1O_2$[53]; (C) Construction of NU-1012 via metal incorporation for generation of $\bullet O_2^-$[41]; (D) Construction of AuNR@ZIF-8@AuNCs through photosensitizer load and noble metal deposition for generation of abundant ROS[50].

On account of the high specific surface area and intrinsic porous framework of MOFs, functional components like semiconductors, noble metal nanoparticles and photosensitizers (**Figure 4, bottom**) can be introduced into MOFs to promote photocatalytic antibacterial performance[43,81]. For example, the construction of heterojunctions can effectively address the issues of insufficient light absorption, fast charge carrier recombination and slow redox reactions[85,86]. Recently, Cao et al. encapsulated quantum dots (QDs) onto ZIF-8 to form a nanocomposite (QDs@ZIF-8) by a simple coordination-assisted self-assembly method[52]. The as-prepared

QDs@ZIF-8 shows enhanced antibacterial activity, boosted by the increase in ROS generation-accelerated interfacial electron migration. Additionally, classic inorganic semiconductors such as MoS_2 and Fe_2O_3 have also been selected to construct heterojunctions with MOFs aiming for boosting antibacterial performance[87,88].

In a recent notable example, Xie et al. looked to grow covalent organic frameworks (COFs) on ZIF-8 templates for forming an ionic ZIF-8@iCOF nanocomposite. Their study found it kills nearly all bacteria (>99.99%) under visible light irradiation for 15 min [53]. The photoactive experiments reveal that the introduction of COFs improved visible-light absorption and exciton-enhanced transmission in MOFs, and is conducive to the generation of abundant ROS (**Figure 5B**). Through embedding into polyacrylonitrile (PAN), the resultant ZIF-8@iCOF/PAN fibrous membranes also displays strong inactivation against bacteria under sunlight[53]. Wu et al. constructed a core−shell bilayer MOF framework named PB@MOF by growing porphyrin-doped MOFs on Prussian blue (PB)[61]. The as-prepared heterojunction achieves almost complete elimination of bacteria by the combined effects of enhanced ROS and hyperthermia under dual light irradiation[61].

Noble metals, such as Ag, Au, and Pt, are known to possess a surface plasmonic resonance effect at the nanoscale[89]. They are extensively deposited on semiconductor photocatalysts since they can promote visible-light capture and charge carrier separation[90]. For instance, Shang et al. prepared a ZIF-8 nanocomposite with the in-situ insertion of plasmonic Au nanorods (AuNRs) and glutathione-stabilized Au nanoclusters (AuNCs) decoration to yield AuNR@ZIF-8@AuNCs [50]. The plasmon-enhanced effect of AuNRs and the photosensitive action of AuNCs synergistically trigger more ROS production, making the nanocomposites highly efficacious in bacteria inactivation (**Figure 5D**). In addition, fibrous facial masks loaded with these nanocomposites exhibited better antibacterial effect than commercial surgical masks[50], confirming the opportunity for the fabrication of PPE.

Low-cost Ag nanoparticles (AgNPs) are commonly applied as antibacterial agents[2]. Recently, Luo et al. designed an antibacterial nanocomposite by depositing

AgNPs onto NH_2-MIL-125(Ti), denoted as Ag/NM125[66]. Compared with pristine NH_2-MIL-125(Ti) (5.8-log), the nanocomposite exhibits a reduction of more than 7-log *E. coli*. From the perspective of mechanism, the introduction of AgNPs enables Ag/NM125 stronger visible-light capture and quicker charge carrier transfer. Furthermore, the well-dispersed nature of AgNPs on MOFs also enables remarkable antibacterial behavior in the absence of light [66].

To increase the light absorption of photocatalysts, one of the most convenient and effective solutions is to load photosensitizers into the chosen catalyst [91]. For example, Lin et al. encapsulated classic porphyrin photosensitizer onto UiO-66-$(SH)_2$ along with Ag NPs for improving light absorption (UiO-66-$(SH)_2$@TCPP@AgNPs)[62]. The resultant nanocomposite has remarkable bacteria-killing properties, as a result of the availability of sufficient amounts of ROS. ROS generation is enhanced through stronger visible-light capture by the porphyrin doping, and inhibition of charge carrier recombination by Ag NP deposition [62]. In a similar example, Pal et al. loaded hydrophobic squaraine dyes (SQ) onto ZIF-8 to construct ZIF8-SQ[51]. The resultant nanoconjugates show outstanding lethality against methicillin-resistant *S. aureus* (MRSA) under red-light irradiation, attributed to the abundant photoinduced ROS formed by the synergistic effect of photosensitive SQ and porous ZIF-8[51].

Overall, many efforts have been made to improve the photocatalytic antibacterial performance of MOFs. In general, these design strategies are based on promoting quick and efficient generation of ROS and enhancing the binding interaction between the MOFs and bacteria. Nevertheless, there is a high demand for the design and construction strategies to develop functional MOF-based composites, which largely determine the feasibility of their applications in real life.

Concluding remarks and outlook

This review summarizes various intriguing findings about MOF-based materials for photocatalytic sterilization. Thanks to their nanoporous nature, readily-modified structure and tunable functionality, photoactive MOFs are emerging as desirable platforms for photocatalytic antimicrobial applications. Additionally, characterization

techniques such as single-crystal X-ray diffraction can be used to accurately analyze the crystal structure of MOFs, which allows researchers to understand the relationship between the structure, properties and functions of MOFs in detail. However, it remains a challenge to employ MOF-based materials as state-of-the-art antibacterial weapons in real-life situations, as noted by the limited number of applications demonstrated in the discussed examples. Looking forward, it is clear there are many open opportunities for the development of MOF-based photocatalytic antibacterial applications in three aspects, namely structural design, MOF-based composites, and photocatalytic antimicrobial methods.

Structural design

It remains a difficult task to design and construct ideal MOF-based photocatalysts owing to the need to comprehensively consider their functionality, stability, and biosafety together [2,6]. MOF-based photocatalysts can generally absorb ultraviolet and visible light, but they rarely utilize the full spectrum of sunlight[2]. One suggestion here is to combine machine learning and big data analysis for high-throughput experimental screening of near-infrared-driven and biofriendly MOFs[92-94]. In addition, bacteria-killing MOF-based photocatalysts with visual indicators for antibacterial performance would be valuable in practical scenarios[60]. MOFs with the ability to readily incorporate diverse handles and moieties can enable the introduction of fluorescent molecules, and this concept can facilitate the implementation of an integrated system for visual identification, bacterial inactivation, and evaluation[60].

The stability, flexibility, durability, service life as well as the overall robustness of MOF-based composites in practical applications are of much concern[21]. It is a prerequisite to design stable MOFs on the basis of reticular chemistry and the principle of HSAB for building up a robust combination of MOFs and substrates via supramolecular interactions [23,46]. Furthermore, biosafety should be given the top priority when MOFs are intended to be applied for biomedical and healthcare applications. It is preferrable to design biosafe MOFs through the combination of biocompatible organic ligands and endogenous metal components[16,95]. Also,

cytotoxicity assessment of MOFs should be performed to ensure good biocompatibility, which promotes the construction of a standardized antimicrobial evaluation system and enables the comparison between different antimicrobial materials.

Large-scale production of high-efficiency MOF-based composites

The scalability, processability and applicability of MOFs is also important in terms of practical antibacterial applications[80,96]. MOFs are commonly prepared by solvothermal reactions in a laboratory scale with limited yield. Recently-emerging methods such as electrochemical synthesis, ultrasonic synthesis and microwave synthesis could potentially be used for the scalable manufacture of antibacterial MOFs[97,98]. Additionally, protective clothing and equipment fabricated with sustainable MOF-based composites are in high demand, and the use of environmental-friendly and biodegradable supporting substrates, such as lignocellulose, bacterial cellulose and cotton fabrics, are favorable[99,100].

There is an urgent need to search for new strategies to improve photocatalytic antimicrobial efficiency of MOFs for diverse antibacterial application scenarios and specific antibacterial functions [2,6]. New insights like introducing a piezoelectric effect and an external electric field in MOF-based composites have been recently reported for their feasibility in constructing high-performance photocatalytic antibacterial materials[43]. Also, it has been reported that defects and particle sizes of MOFs can be tuned for optimizing catalytic performance[45], which may be attractive methods for the regulation of photocatalytic antibacterial activity.

Photocatalytic antimicrobial methods

Phototherapy based on photogenerated ROS can effectively fight against multidrug-resistant microbes, but may also influence the production of antioxidant enzymes in microorganisms, because of the reduction of ROS accumulated in microbial cells[2]. Stabilizing the accumulation of intracellular ROS by precisely controlling various parameters can be an efficacious solution, which requires further exploration. Besides, the photocatalytic process is often accompanied by a photothermal effect, also called photothermal therapy (PTT). Therefore, a sound evaluation system should be

established to distinguish the effects of photogenerated ROS and photogenerated heat on antibacterial performance, clarifying whether the antibacterial ability is a result of single effect or synergistic effect[16,31]. Additionally, strong oxidative ROS unselectively inactivate versatile bad and good microbes[2,6,84]. It is necessary to regulate different parameters like the intensity of light source and radiation time for various antimicrobial effects as well as build a targeted action system with MOFs for specific scenarios or applications.

Acknowledgement

Z. C. gratefully acknowledges support by the National Natural Science Foundation of China (Grant No. 22201247) and the startup funding from Zhejiang University. We thank the staff at BL17B1 beamline of the National Facility for Protein Science in Shanghai (NFPS), Shanghai Advanced Research Institute, CAS, for providing technical support in X-ray diffraction data collection and analysis. We thank the Chemistry Instrumentation Center Zhejiang University for the technical support. K. M. acknowledges the support from the start-up fund of the Hong Kong Polytechnic University (1-BDD2) and ESG Hub 1-WZ2H.

Declaration of interests

No interests are declared.

References

1. Wu, Y. *et al.* (2024) Interdisciplinary-inspired smart antibacterial materials and their biomedical applications. *Adv. Mater.* 36, e2305940.
2. Ran, B. *et al.* (2023) Photocatalytic antimicrobials: Principles, design strategies, and applications. *Chem. Rev.* 123, 12371-12430.
3. Bloom, D. E. and Cadarette, D. (2019) Infectious disease threats in the twenty-first century: Strengthening the global response. *Front. Immunol.* 10, 549.
4. Li, J. *et al.* (2023) Electroactive materials: Innovative antibacterial platforms for biomedical applications. *Prog. Mater. Sci.* 132, 101045.
5. Ganguly, P. *et al.* (2018) Antimicrobial activity of photocatalysts: Fundamentals, mechanisms, kinetics and recent advances. *Appl. Catal. B-Environ.* 225, 51-75.
6. Zeng, J. *et al.* (2021) Progress on photocatalytic semiconductor hybrids for

bacterial inactivation. *Mater. Horiz.* 8, 2964-3008.
7. Wang, Q. and Astruc, D. (2020) State of the art and prospects in metal-organic framework (MOF)-based and MOF-derived nanocatalysis. *Chem. Rev.* 120, 1438-1511.
8. Shi, L. *et al.* (2024) Quasicrystal approximants in isoreticular metal-organic frameworks via cairo pentagonal tiling. *Chem* 10, 1-9.
9. Shi, L. *et al.* (2024) A hetero-supermolecular-building-block strategy for the assembly of porous (3,12,24)-connected uru metal-organic frameworks. *Nat. Synth.* https://doi.org/10.1038/s44160-024-00622-5.
10. Tang, J. *et al.* (2023) Metal-organic framework nanoshell structures: Preparation and biomedical applications. *Coord. Chem. Rev.* 490, 215211-215258.
11. Yang, J. and Yang, Y. W. (2020) Metal-organic frameworks for biomedical applications. *Small* 16, e1906846.
12. Cai, G. *et al.* (2021) Metal-organic framework-based hierarchically porous materials: Synthesis and applications. *Chem. Rev.* 121, 12278-12326.
13. Feng, L. *et al.* (2019) Controllable synthesis of metal-organic frameworks and their hierarchical assemblies. *Matter* 1, 801-824.
14. Zhang, X. *et al.* (2020) Design and applications of water-stable metal-organic frameworks: Status and challenges. *Coord. Chem. Rev.* 423, 213507-213528.
15. Li, R. *et al.* (2021) Metal-organic-framework-based materials for antimicrobial applications. *ACS Nano* 15, 3808-3848.
16. Han, D. *et al.* (2022) Metal organic framework-based antibacterial agents and their underlying mechanisms. *Chem. Soc. Rev.* 51, 7138-7169.
17. Ren, Y. *et al.* (2020) Photoresponsive materials for antibacterial applications. *Cell Rep. Phys. Sci.* 1, 100245.
18. Wang, Y. *et al.* (2022) Chemically engineered porous molecular coatings as reactive oxygen species generators and reservoirs for long-lasting self-cleaning textiles. *Angew. Chem. Int. Ed.* 61, e202115956.
19. Cheung, Y. H. *et al.* (2021) Immobilized regenerable active chlorine within a zirconium-based MOF textile composite to eliminate biological and chemical threats. *J. Am. Chem. Soc.* 143, 16777-16785.
20. Kalaj, M. *et al.* (2020) MOF-polymer hybrid materials: From simple composites to tailored architectures. *Chem. Rev.* 120, 8267-8302.
21. Ma, K. *et al.* (2020) Fiber composites of metal-organic frameworks. *Chem. Mater.* 32, 7120-7140.
22. Peterson, G. W. *et al.* (2021) Fibre-based composites from the integration of metal-organic frameworks and polymers. *Nat. Rev. Mater.* 6, 605-621.
23. Tu, K. *et al.* (2022) Review on design strategies and applications of metal-organic framework-cellulose composites. *Carbohydr. Polym.* 291, 119539.
24. Eagleton, A. M. *et al.* (2023) Fiber integrated metal-organic frameworks as functional components in smart textiles. *Angew. Chem. Int. Ed.* 62, e202309078.
25. Ma, K. *et al.* (2023) Protection against chemical warfare agents and biological threats using metal-organic frameworks as active layers. *Acc. Mater. Res.* 4, 168-179.

26. Qian, Q. *et al.* (2020) MOF-based membranes for gas separations. *Chem. Rev.* 120, 8161-8266.
27. Wang, D. and Li, T. (2023) Toward MOF@polymer core-shell particles: Design principles and potential applications. *Acc. Chem. Res.* 56, 462-474.
28. Nosaka, Y. and Nosaka, A. Y. (2017) Generation and detection of reactive oxygen species in photocatalysis. *Chem. Rev.* 117, 11302-11336.
29. Zhang, Z. *et al.* (2022) Porous organic polymers for light-driven organic transformations. *Chem. Soc. Rev.* 51, 2444-2490.
30. Zhu, S.-S. *et al.* (2024) Recent progress on covalent organic frameworks for photocatalytic hydrogen generation via water splitting. *Mater. Chem. Front.* 8, 1513-1535.
31. Zheng, Q. *et al.* (2021) The recent progress on metal-organic frameworks for phototherapy. *Chem. Soc. Rev.* 50, 5086-5125.
32. Kong, X. *et al.* (2021) Graphitic carbon nitride-based materials for photocatalytic antibacterial application. *Mat. Sci. Eng. R.* 145, 100610.
33. Han, D. *et al.* (2020) Enhanced photocatalytic activity and photothermal effects of Cu-doped metal-organic frameworks for rapid treatment of bacteria-infected wounds. *Appl. Catal. B-Environ.* 261, 118248.
34. Li, Z. *et al.* (2023) Three-component donor-π-acceptor covalent-organic frameworks for boosting photocatalytic hydrogen evolution. *J. Am. Chem. Soc.* 145, 8364-8374.
35. Ma, S. *et al.* (2022) Photocatalytic hydrogen production on a sp^2 -carbon-linked covalent organic framework. *Angew. Chem. Int. Ed.* 61, e202208919.
36. García-Baldoví, A. *et al.* (2023) Active site imprinting on Ti oxocluster metal-organic frameworks for photocatalytic hydrogen release from formic acid. *Energy Environ. Sci.* 16, 167-177.
37. Liang, R. *et al.* (2015) M@MIL-100(Fe) (m = Au, Pd, Pt) nanocomposites fabricated by a facile photodeposition process: Efficient visible-light photocatalysts for redox reactions in water. *Nano Res.* 8, 3237-3249.
38. Chen, M. *et al.* (2022) Boronic acid-decorated multivariate photosensitive metal-organic frameworks for combating multi-drug-resistant bacteria. *ACS Nano* 16, 7732-7744.
39. Li, P. *et al.* (2019) Metal-organic frameworks with photocatalytic bactericidal activity for integrated air cleaning. *Nat. Commun.* 10, 2177.
40. Chen, M. *et al.* (2020) Titanium incorporation into Zr-porphyrinic metal-organic frameworks with enhanced antibacterial activity against multidrug-resistant pathogens. *Small* 16, e1906240.
41. Wang, X. *et al.* (2022) Photocatalytic biocidal coatings featuring Zr_6Ti_4-based metal-organic frameworks. *J. Am. Chem. Soc.* 144, 12192-12201.
42. Luo, Y. *et al.* (2022) Simultaneously enhancing the photocatalytic and photothermal effect of NH_2-MIL-125-GO-Pt ternary heterojunction for rapid therapy of bacteria-infected wounds. *Bioact. Mater.* 18, 421-432.
43. Sun, K. *et al.* (2023) Metal-organic frameworks for photocatalytic water splitting and CO_2 reduction. *Angew. Chem. Int. Ed.* 62, e202217565.

44. Qian, Z. *et al.* (2023) Trace to the source: Self-tuning of MOF photocatalysts. *Adv. Energy Mater.* 13, 2300086.
45. Shi, L. *et al.* (2023) Design, synthesis and applications of functional zirconium-based metal-organic frameworks. *Sci. China Chem.* 66, 3383-3397.
46. Chen, Z. *et al.* (2023) Rational design of stable functional metal-organic frameworks. *Mater. Horiz.* 10, 3257-3268.
47. Cai, X. *et al.* (2023) MOF-integrated hierarchical composite fiber for efficient daytime radiative cooling and antibacterial protective textiles. *ACS Appl. Mater. Interfaces* 15, 8537-8545.
48. Wang, Z. *et al.* (2021) Epitaxially grown MOF membranes with photocatalytic bactericidal activity for biofouling mitigation in desalination. *J. Membrane Sci.* 630, 119327-119338.
49. Wang, C. *et al.* (2022) The enhanced photocatalytic sterilization of MOF-based nanohybrid for rapid and portable therapy of bacteria-infected open wounds. *Bioact. Mater.* 13, 200-211.
50. Guo, W. *et al.* (2023) Plasmon-enhanced visible-light photocatalytic antibacterial activity of metal-organic framework/gold nanocomposites. *J. Mater. Chem. A* 11, 2391-2401.
51. Bagchi, D. *et al.* (2019) Nano MOF entrapping hydrophobic photosensitizer for dual-stimuli-responsive unprecedented therapeutic action against drug-resistant bacteria. *ACS Appl. Bio Mater* 2, 1772-1780.
52. Wang, M. *et al.* (2021) Encapsulation of colloidal semiconductor quantum dots into metal-organic frameworks for enhanced antibacterial activity through interfacial electron transfer. *Chem. Eng. J.* 426, 130832-130847.
53. Li, Y. *et al.* (2023) Structural engineering of ionic MOF@COF heterointerface for exciton-boosting sunlight-driven photocatalytic filter. *ACS Nano* 17, 2932-2942.
54. Zhang, J. *et al.* (2020) Aluminum metal-organic frameworks with photocatalytic antibacterial activity for autonomous indoor humidity control. *ACS Appl. Mater. Interfaces* 12, 46057-46064.
55. Ma, D. *et al.* (2020) A hydrolytically stable vanadium(iv) metal-organic framework with photocatalytic bacteriostatic activity for autonomous indoor humidity control. *Angew. Chem. Int. Ed.* 59, 3905-3909.
56. Zhao, Y. *et al.* (2024) Versatile multi-wavelength light-responsive metal-organic frameworks micromotor through porphyrin metalation for water sterilization. *Small* 20, e2305189.
57. Xue, J. *et al.* (2024) Visible-light-driven Au/PCN-224/Cu(ii) modified fabric with enhanced photocatalytic antibacterial and degradation activity and mechanism insight. *Sep. Purif. Technol.* 333, 125863-125874.
58. Liu, Y. Y. *et al.* (2021) Effect of topology on photodynamic sterilization of porphyrinic metal-organic frameworks. *Chem. Eur. J.* 27, 10151-10159.
59. Zheng, S. *et al.* (2023) PDINH bridged NH_2-UiO-66(Zr) Z-scheme heterojunction for promoted photocatalytic Cr(VI) reduction and antibacterial activity. *J. Hazard Mater.* 447, 130849.

60. Zuo, W. *et al.* (2021) An integrated platform for label-free fluorescence detection and inactivation of bacteria based on boric acid functionalized Zr-MOF. *Sensors Actuat. B-Chem.* 345, 130345-130352.
61. Luo, Y. *et al.* (2019) Dual metal-organic framework heterointerface. *ACS Cent. Sci.* 5, 1591-1601.
62. Xie, B. X. *et al.* (2023) Boosting antibacterial photodynamic therapy in a nanosized Zr MOF by the combination of Ag NP encapsulation and porphyrin doping. *Inorg. Chem.* 62, 13892-13901.
63. Wang, S. *et al.* (2022) PDI bridged MIL-125(Ti)-NH_2 heterojunction with frustrated Lewis pairs: A promising photocatalyst for Cr(VI) reduction and antibacterial application. *Appl. Catal. B-Environ.* 317, 121798-121810.
64. Yu, G. *et al.* (2022) Boosting reactive oxygen species generation by regulating excitonic effects in porphyrinic covalent organic frameworks. *J. Phys. Chem. Lett.* 13, 2814-2823.
65. Fu, Y. *et al.* (2023) Fabrication of wide-spectra-responsive NA/NH_2-MIL-125(Ti) with boosted activity for Cr(VI) reduction and antibacterial effects. *Chem. Eng. J.* 452, 139417-139427.
66. Sun, X. *et al.* (2023) Ag Nanoparticle and Ti-MOF Cooperativity for Efficient Inactivation of E. coli in Water. *ACS Appl. Mater. Interfaces* 15, 43712-43723.
67. Wu, R. *et al.* (2019) Synthetic factors affecting the scalable production of zeolitic imidazolate frameworks. *Acs Sustain. Chem. Eng.* 7, 3632-3646.
68. Liao, P. Q. *et al.* (2015) Efficient purification of ethene by an ethane-trapping metal-organic framework. *Nat. Commun.* 6, 8697.
69. Liu, Y. *et al.* (2021) The application of zeolitic imidazolate frameworks (ZIFs) and their derivatives based materials for photocatalytic hydrogen evolution and pollutants treatment. *Chem. Eng. J.* 417, 127914-127934.
70. Maleki, A. *et al.* (2020) The progress and prospect of zeolitic imidazolate frameworks in cancer therapy, antibacterial activity, and biomineralization. *Adv. Healthc. Mater.* 9, e2000248.
71. Fan, W. *et al.* (2023) Aluminum metal-organic frameworks: From structures to applications. *Coord. Chem. Rev.* 489, 215175-215214.
72. Zhu, J. *et al.* (2022) Vanadium-based metal-organic frameworks and their derivatives for electrochemical energy conversion and storage. *SmartMat* 3, 384-416.
73. Gupta, S. (2023) Recent reports on vanadium based coordination polymers and MOFs. *Rev. Inorg. Chem.* 43, 465-493.
74. Chen, Z. *et al.* (2019) Reticular chemistry in the rational synthesis of functional zirconium cluster-based MOFs. *Coord. Chem. Rev.* 386, 32-49.
75. Feng, L. *et al.* (2020) Strategies for pore engineering in zirconium metal-organic frameworks. *Chem* 6, 2902-2923.
76. Li, J. *et al.* (2023) Zr- and Ti-based metal-organic frameworks: Synthesis, structures and catalytic applications. *Chem. Commun.* 59, 2541-2559.
77. Jiang, H. *et al.* (2023) Planar chiral [2.2]paracyclophane-based Zr(iv) metal-organic frameworks. *CCS Chem.* 5, 1635-1643.

78. Shi, L. *et al.* (2024) Metal-organic frameworks for water vapor adsorption. *Chem* 10, 484-503.
79. Bai, Y. *et al.* (2016) Zr-based metal-organic frameworks: Design, synthesis, structure, and applications. *Chem. Soc. Rev.* 45, 2327-2367.
80. Drout, R. J. *et al.* (2019) Zirconium metal-organic frameworks for organic pollutant adsorption. *Trends Chem.* 1, 304-317.
81. Banerjee, S. *et al.* (2020) Biomedical integration of metal-organic frameworks. *Trends Chem.* 2, 467-479.
82. Zhu, J. *et al.* (2018) Titanium-based metal-organic frameworks for photocatalytic applications. *Coord. Chem. Rev.* 359, 80-101.
83. Chen, J. *et al.* (2022) Recent advances in Ti-based MOFs in biomedical applications. *Dalton Trans.* 51, 14817-14832.
84. Wang, W. *et al.* (2021) Carbon nitride based photocatalysts for solar photocatalytic disinfection, can we go further? *Chem. Eng. J.* 404, 126540-126562.
85. Zhu, B. *et al.* (2024) Construction of 2D S-scheme heterojunction photocatalyst. *Adv. Mater.* 36, e2310600.
86. Tsao, C.-W. *et al.* (2021) Modulation of interfacial charge dynamics of semiconductor heterostructures for advanced photocatalytic applications. *Coord. Chem. Rev.* 438, 213876-213905.
87. Yang, Z. *et al.* (2023) A core-shell 2D-MoS_2@MOF heterostructure for rapid therapy of bacteria-infected wounds by enhanced photocatalysis. *Chem. Eng. J.* 451, 139127-139143.
88. Li, J. *et al.* (2022) Atomic-layer Fe_2O_3-modified 2D porphyrinic metal-organic framework for enhanced photocatalytic disinfection through electron-withdrawing effect. *Appl. Catal. B-Environ.* 317, 121701-121714.
89. Wang, M. *et al.* (2016) Plasmon-mediated solar energy conversion via photocatalysis in noble metal/semiconductor composites. *Adv. Sci.* 3, 1600024.
90. Kavitha, R. *et al.* (2020) Noble metal deposited graphitic carbon nitride based heterojunction photocatalysts. *Appl. Surf. Sci.* 508, 145142-145163..
91. Kim, D. *et al.* (2023) Improved transition metal photosensitizers to drive advances in photocatalysis. *Chem. Sci.* 15, 77-94.
92. Yang, H. *et al.* (2023) Machine learning accelerated exploration of ternary organic heterojunction photocatalysts for sacrificial hydrogen evolution. *J. Am. Chem. Soc.* 145, 27038-27044.
93. Zheng, Z. *et al.* (2023) ChatGPT chemistry assistant for text mining and the prediction of MOF synthesis. *J. Am. Chem. Soc.* 145, 18048-18062.
94. Zheng, Z. *et al.* (2023) Shaping the water-harvesting behavior of metal-organic frameworks aided by fine-tuned GPT models. *J. Am. Chem. Soc.* 145, 28284-28295.
95. Kumar, S. *et al.* (2020) Green synthesis of metal-organic frameworks: A state-of-the-art review of potential environmental and medical applications. *Coord. Chem. Rev.* 420, 213407-213433.
96. Yan, L. *et al.* (2022) Metal organic frameworks for antibacterial applications.

Chem. Eng. J. 435, 134975-134989.
97. Li, Y. *et al.* (2022) Synthesis and shaping of metal-organic frameworks: A review. *Chem. Commun.* 58, 11488-11506.
98. Khalil, I. E. *et al.* (2023) Tackling orientation of metal-organic frameworks (MOFs): The quest to enhance MOF performance. *Coord. Chem. Rev.* 481, 215043-215074.
99. Etale, A. *et al.* (2023) Cellulose: A review of water interactions, applications in composites, and water treatment. *Chem. Rev.* 123, 2016-2048.
100. Lu, Y. *et al.* (2022) Recent advances in metal organic framework and cellulose nanomaterial composites. *Coord. Chem. Rev.* 461, 214496-214529.